Original Article

Steady-state analysis of suitable interconnection points for integration of offshore wind farms in the Gulf of Thailand♣

Kusumal Chalermyanont* and Phichet Ketsamee

Department of Electrical Engineering, Faculty of Engineering,
Prince of Songkla University, Hat Yai, Songkhla, 90112 Thailand

Abstract

In Thailand, there is great potential for large-scale offshore wind farms in the Gulf of Thailand between Koh Tao and Koh Pha-Ngan, with possible installed capacity of up to 432 MW. The integration of large-scale wind farms will significantly impact the stability, security, quality, and operation of the power grid. In this paper, possible interconnection points to the 115-kV distribution grid system of the Provincial Electricity Authority (PEA) are selected for integrating three offshore wind farms. The steady-state analysis of power flows, voltage variations, voltage stability, and fault currents is performed using the DIgSILENT Power Factory program. The simulation results indicate appropriate interconnection points for offshore wind farms to the 115-kV grid. These results will be important for developing offshore wind farms in Thailand.

Keywords: large-scale wind farm, interconnection point, fault currents, power flows, voltage stability, voltage variations, Gulf of Thailand

1. Introduction

Emphasis on the use of wind energy has strongly increased worldwide. Offshore wind farms are currently gaining attention because of the abundance of wind resources that could be developed into large-scale energy resources in unlimited installation areas. The annual report of Global Wind Energy Council, 2020, found that offshore wind energy installed capacity was about 6.1 GW in 2019, bringing the total global cumulative installations to 29.1 GW. In Thailand, the Alternative Energy Situation reports that, in 2019, the total capacity of wind energy reached approximately 1.50 GW, but all of this was onshore type of wind farms. Additionally, it is forecast that in 2030 more than 205 GW of new offshore wind capacity will have been added globally (Global Wind Energy Council, 2020).

The mesoscale wind map at 100 m asl for the gulf of Thailand shown in Figure 1 indicates high potential for large-
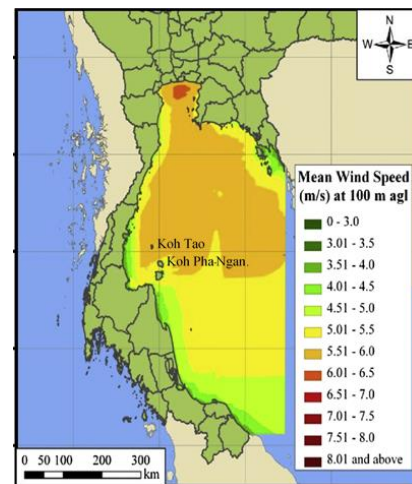
Figure 1. Mesoscale wind map at 100 m asl for the Gulf of Thailand (Waewsak, Landry, & Gagnon, 2015)

scale offshore wind farms between Koh Tao and Koh Pha-Ngan (Waewsak, Landry, & Gagnon, 2015). However, no feasibility study has yet assessed the appropriate choices of

interconnection points for the offshore wind farms to the grid. Ketsamee, Chalermyanont, and Prasertsit, (2015), estimated the installation capacity of offshore wind farms in that area as about 432 MW. This capacity can be composed of three small power producer (SPP) offshore wind farms, labeled as SPP 1, SPP 2, and SPP 3, with 108 MW, 162 MW, and 162 MW, respective capacities. Figure 2 shows approximate locations and installation capacities of the three proposed offshore wind farms and possible 115-kV connection points for the PEA.

Since large-scale offshore wind farms significantly affect the grid operations, the grid's security, stability, and quality have to be analyzed following the general grid connection design of the power system. Evaluating appropriate interconnection points to the grid is required, based on specific grid codes, capacities of the wind farms, and load conditions. Commonly, steady-state systems analyses of power flows (Andersson, Petersson, Agneholm, & Karlsson, 2007; Bhumkittipich & Jan-Ngurn, 2013; Wu, Lee, Chou, & Liao, 2013; Wu, Han, & Lee, 2013; Wu, Lee, Chao, & Chang, 2010; Wu, Lee, & Shu, 2011; Zamora & Rosado, 2014), voltage variations (Wu *et al.*, 2011, 20130), voltage stability (Bhumkittipich *et al.*, 2013; Linh. & Chuong, 2009; Said, Aly, & Abdek-Akher, 2013; Zamora *et al.*, 2014) and fault currents (Andersson *et al.*, 2007; Wu *et al.*, 2010, 2011, 2013; Wu, Lee, Chen, & Tsai, 2011) are performed to assess suitable connection points for offshore wind farm integration.

In this paper, possible existing interconnection points to the 115-kV distribution grid system of PEA are selected for integrating the three proposed offshore wind farms (SPP1-SPP3). The steady-state analyses of power flows, voltage variations, voltage stability, and fault currents are performed under Thailand grid connection requirements for renewable energy, as explained in Section II. Section III describes the system data of possible buses of 115-kV grid system during peak and off-peak load conditions. The simulation is performed using the DIgSILENT Power Factory program, and the analytical results are shown in Section IV. Finally, suitable interconnection points for the three offshore wind farms are described in Section V.

2. Grid Connection Requirements for the Renewable Energy in Thailand

The electricity system operators in Thailand, such as the Electricity Generating Authority of Thailand (EGAT) and the Provincial Electricity Authority (PEA), define renewable energy grid connection requirements for all parties to maintain security and stability, and power quality of the power system. The steady-state analyses necessary consider the following requirements.

2.1 Power flow analysis

The integration of offshore wind farms will affect power flow directions and power losses in the grid. According to the grid requirement of EGAT, electric power is not allowed to flow back to HV-substations of EGAT utility grid. Moreover, based on PEA grid codes, the power flow must not exceed 80% of the transmission line capacity during regular operation. The power flow analysis can also assess power losses in the power system after connecting offshore wind farms.

Figure 2.   The approximate locations and installation capacities of offshore wind farms and the 115-kV PEA buses: SMA, SMB, and KCD

2.2 Voltage variation analysis

When the offshore wind farms are integrated into the grid, normal voltage variations at connected points must remain within ± 5%. Furthermore, the standard system voltage range should be maintained between 109.2 kV and 120.7 kV or from 0.95 p.u. to 1.05 p.u.

2.3 Voltage stability analysis

In practice, voltage stability is not among the grid requirements for interconnections of offshore wind farms. However, the additional power from offshore wind farms can impact voltage stability in the power system. Therefore, in this paper, a new voltage stability calculation is done because it can indicate the grid's critical points, which must have a voltage collapse coefficient less than 0.2 (Gregor & Ferdinand, 2002). Moreover, the results can be used to design additional protection equipment for the power system.

2.4 Fault current analysis

Fault current calculations with offshore wind farms connected to the grid help assess whether existing protective equipment remain sufficient, or support selecting appropriate ratings for new protective devices. Based on the Provincial Electricity Authority (PEA) requirements for power system interconnections, fault current level must be less than 85% of the original circuit breaker's interruption capacity (I.C.). Therefore, it is not allowed to exceed by 25% the system without offshore wind farms.

3. System Description

The large-scale offshore wind farms of SPP1, SPP2, and SPP3 described above are connected to the 115 kV

transmission system following the connection requirements of renewable energy generation above 10 MW of PEA, which is based on physical criteria, such as amount of transformers, loads, and transmission line distances to the connection points. The three possible connected buses for integrating offshore wind farms are Koh Samui A (KMA-bus), Koh Samui B (KMB-bus), and Kanchanadit (KCD -bus), shown in the single line diagram of Figure 3. Each point is connected to the buses KN3, KN1, and KN2 of EGAT, respectively. The data on possible connected buses under peak and off-peak load conditions from PEA are shown in Table 1.
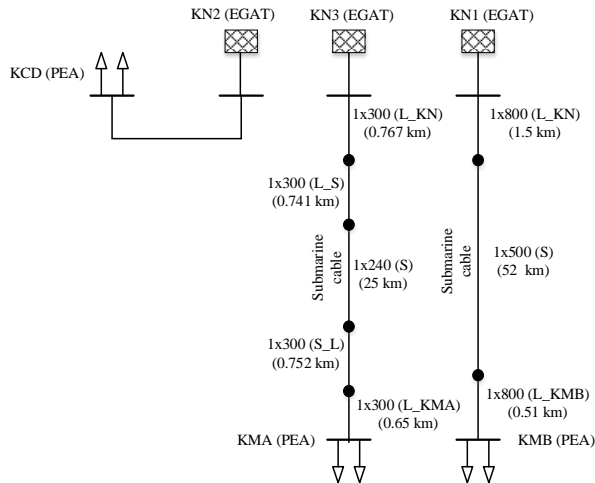
Figure 3. A single line diagram of possible interconnection points for integrating offshore wind farms in the Gulf of Thailand

The full-power conversion wind turbine generator of Vestas (V112 model) with a 3-MW rating is used in this paper. However, the power from each wind turbine has to be adjusted using the capacity factor (C.F.). Figure 4 shows each offshore wind farm's aggregation model connected to the 33 /115 kV transformer and connected to the grid via submerged cables. The distances between wind farms and connection points are listed in Table 2.

4. Results of the System Simulation

The grid-connection points of offshore wind farms must be appropriately chosen to ensure that electric energy
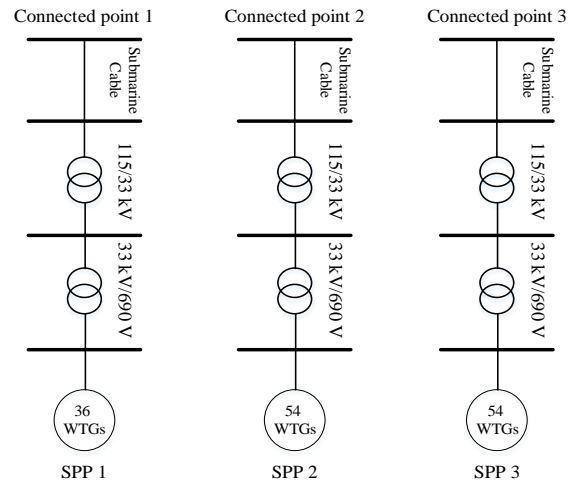
Figure 4. The aggregation model of each offshore wind farm

Table 2. The distances between offshore wind farms and connection points

Offshore wind farm topologies	Distance (km)		
	SPP 1	SPP 2	SPP 3
KMA	87.93	62.26	46.14
KMB	72.43	46.38	31.25
KCD	-	92.75	79.58

can be transmitted to customers regularly and reliably. The impacts on the system depend on grid behavior and on the offshore wind farms, specifically locations of offshore wind farms, wind generator types, and correlation between wind power production and load consumption (Said et al., 2013). In this paper, four possible connection configurations for the three offshore wind farms are proposed in Table 3. Case study 0, with no offshore wind farm connected, is used as the reference case. The peak and off-peak load data provided from PEA are used to analyze the steady state of the power system. The steady-state analyses of power flow, voltage variation, voltage stability, and fault currents, are performed under the wind power integrated operation rules of PEA. The DIgSILENT Power Factory program is utilized to investigate the system impacts.

Table 1. The data on possibly connected buses under peak and off-peak load conditions

Bus	Type	V (p.u.)	Angle (degree)	Load		Generation	
				(MW)	(MVAR)	(MW)	(MVAR)
KN 1	Slack(Peak)	1.040/	0.000	0.000	0.000	65.280	25.620
	Slack(Off-peak)	1.040	0.000	0.000	0.000	38.850	14.770
KN 2	Slack(Peak)	1.014	0.000	0.000	0.000	49.980	27.140
	Slack(Off-peak)	1.014	0.000	0.000	0.000	29.680	13.980
KN 3	Slack(Peak)	1.023	0.000	0.000	0.000	45.760	15.560
	Slack(Off-peak)	1.023	0.000	0.000	0.000	27.320	9.170
KMA	PQ(Peak)	1.008	-0.532	45.200	14.900	0.000	0.000
	PQ(Off-peak)	1.014	-0.317	27.120	8.940	0.000	0.000
KMB	PQ(Peak)	1.010	-1.501	64.000	23.200	0.000	0.000
	PQ(Off-peak)	1.022	-0.889	38.400	13.920	0.000	0.000
KCD	PQ(Peak)	0.955	-3.970	48.800	24.500	0.000	0.000
	PQ(Off-peak)	0.981	-2.328	29.280	14.700	0.000	0.000

Table 3.   The offshore wind farm connection configurations

Case studied	Offshore wind farm connections		
	SPP 1	SPP 2	SPP 3
0	-	-	-
1	KMA	KMB	KCD
2	KMA	KCD	KMB
3	KMB	KMA	KCD
4	KMB	KCD	KMA

4.1 Results on power flow

The 432-MW from three offshore wind farms is integrated into the grid under peak and off-peak load conditions. The power directions and percentages of load in transmission lines are observed. The load percentages of transmission lines under both peak load and off-peak load conditions are presented in Table 4. The simulation results show no power flowing back to the EGAT utility grid in any of the cases. Moreover, the loads in transmission lines between PEA and EGAT buses are below 80% and decreased compared to case study 0 in both peak load and off-peak load conditions, except in case studies 3 and 4 of off-peak load conditions in KMA bus. This means that load power on the grid is supported by offshore wind farms. As a result, the load percentages in the transmission lines decreased. Moreover, the results can be effectively improved if higher capacity offshore wind farms are installed within shorter transmission distances.

Table 5 presents the grid power losses in each study case when the wind farms are connected. The power losses of the system depend on location of the connection point and on difference between power generation of offshore wind farms and load on the grid. For example, the grid loss of case study

1 is lower than in the other cases because the offshore wind farms, in this case, are connected near the center load. Moreover, under off-peak load conditions, the power loss of the power system is higher than that in peak load conditions because of the large difference between the power load and power generation of offshore wind farms.

4.2 Results on voltage variation

The voltage variation analysis was carried out based on two operating modes: voltage control mode and power factor control mode. Also, alternative control modes of the operation impact the system response at connection points to the wind turbines. For the voltage variation simulation, all offshore wind farms operated in two modes: 1.0 p.u. for both voltage control and power factor control modes. The simulation results indicate that the voltage variation at each connection point is still under 5% in both voltage and power factor control modes, as demonstrated in Tables 6 and 7. The voltage variations under the voltage control mode are shown in Table 7, and voltages at connection points are less than one percent in the power factor control mode of Table 6. The voltage variations are approximately 1.00-1.60% under the power factor control mode, whereas the voltage variations are approximately 0.01-0.30% for the voltage control mode. Therefore, further steady-state analysis used the voltage control mode.

4.3 Results on Voltage Stability

The voltage stability is analyzed to determine the critical voltage of the power system by considering voltage, active power, and reactive power at connection points. It can be represented by the relationship between the P-V curve and

Table 4.   The load percentages of transmission lines under peak and off-peak load conditions

Case studied	Load conditions	Load (%)			Compared with case 0		
		KN3-KMA	KN 1-KMB	KN 2-KCD	KN3-KMA	KN 1-KMB	KN 2-KCD
0	Peal	46.490	55.040	33.580	-	-	-
	Off-peak	27.720	32.620	19.620	-	-	-
1	Peak	39.900	46.610	23.960	-14.175	-15.316	-28.648
	Off-peak	27.260	30.400	15.120	-1.659	-6.806	-22.936
2	Peak	39.900	46.620	24.090	-14.175	-15.300	-28.261
	Off-peak	27.260	30.520	15.200	-1.659	-6.438	-22.528
3	Peak	38.570	48.510	23.960	-17.036	-11.864	-28.648
	Off-peak	28.230	30.700	15.120	+1.840	-5.886	-22.936
4	Peak	38.610	48.510	24.090	-16.950	-11.864	-28.261
	Off-peak	28.370	30.700	15.200	+2.345	-5.886	-22.528

Table 5.   The impacts of power loss in the power system

Case studied	Peak load		Off-peak load	
	Power loss (MW)	% Difference compared with case 0	Power loss (MW)	% Difference compared with case 0
0	3.020	-	1.050	-
1	3.020	-	1.980	+88.571
2	3.000	-0.662	1.960	+86.667
3	3.090	+2.318	2.040	+94.286
4	3.070	+1.656	2.010	+91.429

Table 6.   The voltage variation at each connection point under peak and off-peak load conditions in power factor control mode

Case studied	Load conditions	Voltage level (kV)			Voltage variation (%)		
		KMA	KMB	KCD	KMA	KMB	KCD
0	Peak	115.889	116.102	109.794	-	-	-
	Off-peak	116.622	117.537	112.782	-	-	-
1	Peak	117.142	117.240	111.369	+1.081	+0.980	+1.435
	Off-peak	117.863	118.640	114.191	+1.064	+0.938	+1.249
2	Peak	117.142	117.082	111.495	+1.081	+0.844	+1.550
	Off-peak	117.863	118.483	114.316	+1.064	+0.805	+1.360
3	Peak	117.169	117.244	111.369	+1.105	+0.984	+1.435
	Off-peak	117.890	118.647	114.191	+1.087	+0.944	+1.249
4	Peak	117.000	117.244	111.495	+0.959	+0.984	+1.550
	Off-peak	117.721	118.647	114.316	+0.942	+0.944	+1.360

Table 7.   The voltage variation at each connection point under peak and off-peak load conditions in voltage control mode

Case studied	Load conditions	Voltage level (kV)			Voltage variation (%)		
		KMA	KMB	KCD	KMA	KMB	KCD
0	Peak	115.889	116.102	109.794	-	-	-
	Off-peak	116.622	117.537	112.782	-	-	-
1	Peak	115.889	115.818	110.088	+0.009	-0.245	+0.268
	Off-peak	116.578	117.051	112.127	-0.038	-0.413	-0.581
2	Peak	115.899	115.816	110.041	+0.009	-0.246	+0.225
	Off-peak	116.578	117.043	112.099	-0.038	-0.420	-0.606
3	Peak	115.975	115.764	110.088	+0.074	-0.291	+0.268
	Off-peak	116.648	117.018	112.127	+0.022	-0.442	-0.581
4	Peak	115.974	115.764	110.041	+0.073	-0.291	+0.225
	Off-peak	116.645	117.018	112.099	+0.020	-0.442	-0.606

the V-Q curve, which are shown in Figure 5 (a) and (b), respectively. A P-V curve is plotted by increasing the active power in one load or a certain number of loads while keeping the power factor constant. Instability occurs when the load is increased to the point where the currents no longer converge to the load. This point is called the critical point. Generally, an operating point above the critical point implies a stable system, and an operating point below the critical point is considered an unstable system. The power flow usually creates a V-Q curve by keeping the active power constant. The voltage stability limit is at the point where the derivative dQ/dV is zero. This point also defines the minimum reactive power requirement for stable operation. If the operating points are on the right side, the system is diagnosed to be stable. In contrast, if the operating points are on the left side of the critical points, the system is unstable. Additionally, the diagnosis can specify weak bus or high voltage collapse bus and strong bus or low voltage collapse bus by considering the voltage collapse coefficient in Equation 1.

$$k_{cr} = \frac{\sqrt{\left(P_{cr} - P_0\right)^2 + \left(Q_{cr} - Q_0\right)^2}}{\sqrt{\left(P_{cr}\right)^2 + \left(Q_{cr}\right)^2}} \qquad (1)$$

where

P_{cr}, Q_{cr} are active and reactive power at the critical point.

P_{cr}, Q_{cr} are active and reactive power at the starting point.

(a)

(b)
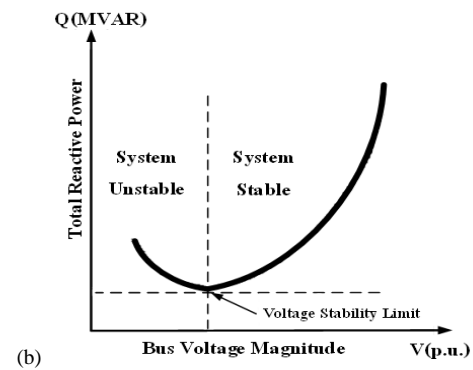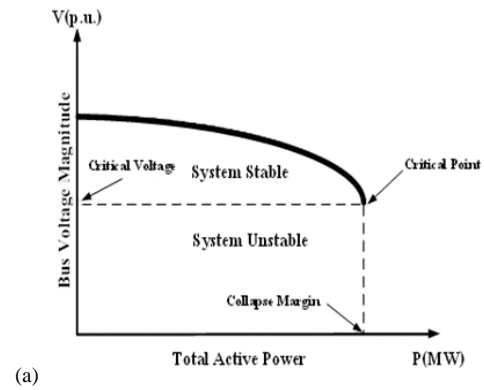
Figure 5.   (a) Schematic of the P-V curve, and (b) of the V-Q curve (Ayodele et al., 2012)

The simulation results of voltage stability at each connected point under peak and off-peak load conditions are summarized in Table 8. When offshore wind farms are connected to the grid, the system can increasingly generate active and reactive power, although the voltage levels decrease. This means that the power system has better voltage stability than one without the offshore wind farm. Consequently, the offshore wind farm can decrease the chance of blackout in the power system.

Additionally, the calculation of the collapse margin coefficient under peak and off-peak load conditions is presented in Table 9. The system with the offshore wind farm has a higher coefficient than one without the offshore wind farm. The coefficient values of all topologies are higher than 0.2, which means that all connection points are be definition solid buses. The offshore wind farm with a shorter distance connection will provide high voltage stability because it can inject high reactive power for compensation voltage level at each connection point. Besides, the larger capacity of the offshore wind farm will also aid higher voltage stability. Moreover, the offshore wind farm connected to the grid under off-peak load conditions gives better voltage stability than the grid under peak load conditions. This is because significant reactive power consumption is needed for the remaining voltage stability in the power system.

4.4 Results of the fault current analysis

The fault current analysis calculates the interrupting current in the system when offshore wind farms are connected to the grid. Moreover, it can evaluate whether the existing protection devices are still usable and is helpful to select appropriate ratings for any new protection devices. In this paper, only a three-phase short circuit analysis is performed to calculate the maximum short circuit currents by using a dynamic voltage support model for full-power conversion wind turbine generator (Nelson, 2012) combined with elements of IEC60909 and G74 standards in an iterative approach (Pöller, M./DIgSILENT GmbH, 2016). The fault current computations at each connected point under peak and off-peak load conditions are summarized in Table 10. The results show that the fault currents remain below the interrupting capacity of the original circuit breakers. As a result, it is not necessary to change the original circuit breakers in this power system. In addition, the current fault

Table 9.   The voltage collapse coefficient under peak and off-peak load conditions

Case	Load conditions	KMA	KMB	KCD
0	Peak	0.9293	0.8526	0.7003
	Off-peak	0.9578	0.9120	0.8193
1	Peak	0.9302	0.8736	0.7711
	Off-peak	0.9600	0.9244	0.8623
2	Peak	0.9302	0.8736	0.7697
	Off-peak	0.9600	0.9244	0.8615
3	Peak	0.9305	0.8715	0.7711
	Off-peak	0.9601	0.9229	0.8623
4	Peak	0.9308	0.8715	0.7697
	Off-peak	0.9602	0.9229	0.8615

level after connecting offshore wind farms is less than 25% relative to the fault current levels without the offshore wind farm integration. It can be concluded that all of the existing circuit breakers are still protecting coordination.

On considering the fault current levels, these levels increased based on the installation capacity of the offshore wind farm. Moreover, the current fault level depends on the length of the transmission line between a connection point and an offshore wind farm because of impedance in the transmission line. Finally, the fault currents under off-peak load conditions are below those under peak load conditions because of lower power load consumption.

The steady-state analytical results of the power flow, voltage variation, voltage stability, and fault current indicate a viable system for operation. Moreover, they can be used to evaluate the capabilities of existing electric power system devices, transmission lines, transformers, and protection devices to support offshore wind power integration into the power grid. The simulation results show that the four possible connection topologies are under PEA grid connection requirements, and there are no negative impacts on the system operation. The summarized steady-state analysis of all cases studied are shown in Table 11.

5. Conclusions

This paper discussed the suitable interconnection points for three offshore wind farms with a total installed capacity of 432 MW. The KMA bus, KMB bus, and KCD bus in 115-kV PEA grid were considered, and four offshore wind

Table 8.   The voltage stability during voltage collapse in peak and off-peak load conditions

Case	KMA			KMB			KCD		
	(p.u.)	(MW)	(MVAR)	(p.u.)	(MW)	(MVAR)	(p.u.)	(MW)	(MVAR)
0 (Peak)	0.695	635.29	222.07	0.71	440.70	136.40	0.648	170.51	41.67
(Off-peak)	0.697	638.05	225.20	0.71	441.41	142.20	0.65	170.73	46.68
1(Peak)	0.677	670.00	237.94	0.66	514.50	155.75	0.579	224.24	59.70
(Off-peak)	0.682	672.77	240.98	0.66	515.14	159.84	0.58	224.26	63.19
2 (Peak)	0.677	670.00	237.94	0.67	514.50	156.60	0.578	222.87	59.13
(Off-peak)	0.682	672.77	240.98	0.67	515.14	160.69	0.58	222.90	62.62
3(Peak)	0.68	670.00	236.375	0.67	505.31	153.64	0.58	224.24	59.71
(Off-peak)	0.681	672.77	242.86	0.67	506.30	157.78	0.58	224.26	63.19
4(Peak)	0.67	670.00	237.155	0.67	505.31	153.64	0.58	222.87	59.13
(Off-peak)	0.691	672.77	243.65	0.67	506.30	157.78	0.58	222.89	62.62

Table 10.   The maximum fault current at each connection point under peak and off-peak load conditions

Case studied	Load conditions	Voltage level (kV)			Fault current variation (%)		
		KMA	KMB	KCD	KMA	KMB	KCD
0	Peak	17.447	13.346	6.431	-	-	-
	Off-peak	17.432	13.328	6.420	-	-	-
1	Peak	17.720	13.680	6.746	+1.565	+2.503	+4.898
	Off-peak	17.708	13.665	6.735	+1.583	+2.529	+4.907
2	Peak	17.720	13.681	6.745	+1.565	+2.510	+4.883
	Off-peak	17.708	13.667	6.734	+1.583	+2.544	+4.891
3	Peak	17.783	13.617	6.746	+1.926	+2.031	+4.898
	Off-peak	17.771	13.602	6.735	+1.945	+2.056	+4.907
4	Peak	17.784	13.617	6.745	+1.932	+2.031	+4.883
	Off-peak	17.772	13.602	6.734	+1.950	+2.056	+4.891

Table 11.   Summary of the steady-state analyses

Case	Power flow	Voltage stability	Voltage variation	Fault current
1	✓	✓	✓	✓
2*	✓	✓	✓	✓
3	✓	✓	✓	✓
4	✓	✓	✓	✓

farm connection cases were proposed. The steady states of power flow, voltage variation, voltage stability, and fault current were simulated and discussed. The results on power flow indicate that power direction and load percentages in the transmission lines satisfy PEA grid connection requirements in all cases studied. In voltage variation analysis, the voltage level was still under control with all offshore wind farm connection cases. The voltage stability results show that collapse margin coefficients for all cases studied at 0.2, and voltage stability can be improved when the offshore wind farms are connected. Finally, the fault current results show that the changed fault current at each connection point was still compatible with the existing circuit breakers.

Based on the steady-state results, all the cases studied of offshore wind farm topologies could support three offshore wind farms and comply with the PEA grid connection requirements. However, in cases 3 and 4, grid losses were higher than in cases 1 and 2. Moreover, in case 1, the transmission line is longer than in case 2. Therefore, the suitable interconnection points of the three offshore wind farms should be as in case 2, with SPP 1 connected to the KMA bus, SPP 2 connected to the KCD bus, and SPP 3 connected to the KMA bus. These results indicate that the 115-kV PEA grid can reliably support large-scale offshore wind farms in the Gulf of Thailand between Koh Tao and Koh Pha-Ngan. In the future, the steady-state analysis for grid integration can be applied to any large-scale renewable power generation and can be useful for developing the actual offshore wind farms in Thailand.

Acknowledgments

References

Andersson, D., Petersson, A., Agneholm, E., & Karlsson, D., (2007). Kriegers Flak 640 MW Offshore wind power grid connection-a real project case study. *IEEE Transaction of Energy Conversion*, *22*(1), 79-85. doi:10.1109/tec.2006.889545.

Ayodele, T. R., Jimoh, A., Munda, J. L., & Tehile, A. J. (2012). Challenges of grid integration of wind power on power system grid integrity: a review. *International Journal of Renewable Energy Research (IJRER)*, *2*(4), 618–626. doi:10.20508/ijrer.87947

Bhumkittipich, K. & Jan-Ngurn, C. (2013). Study of voltage stability for 22 kV power system connected with Lamtakhong wind power plant, Thailand. *Energy Procedia*, *34*, 951-963. doi:10.1016/j.egypro.2013.06.834.

Global Wind Energy Council (2020, June). *GWEC Market intelligence*. Retrieved from https://gwec.net/gwec-market-intelligence-releases-q2-2020-wind-auctions-database/.

Gregor, V., Ferdinand, G. (2002). A novel concept for voltage collapse protection based on local phasors. *IEEE/PES Transmission and Distribution Conference and Exhibition, 1*, 124–129. doi:10.1109/tdc.2002.1178271.

Ketsamee, P., Chalermyanont, K., & Prasertsit, A. (2015). Analysis of suitable interconnection points of offshore wind farms in the Gulf of Thailand. *Energy Procedia*, *79*, 459-464. doi:10.1016/j.egypro.2015.11.519.

Linh, N. T. & Chuong, T. T. (2009). Voltage stability analysis of grids connected wind generators. *Proceedings of the 4th IEEE Conference on Industrial Electronics and Applications, (ICIEA)*, 2657-2660. doi:10.1109/iciea.2009.5138689.

Nelson, R. J. (2012). Short-circuit contributions of full-converter wind turbines. *Proceedings of the 2012 IEEE PES Transmission and Distribution*

Conference and Exposition. doi:10.1109/pes.2011.
6039745.

Pöller, M./DIgSILENT GmbH (2016, July). Modelling of
wind generation for fault level studies, Frankfurt.
Retreived from https://docplayer.net/29105565-
Modelling-of-wind-generation-for-fault-level-
studies-markus-poller-digsilent-gmbh.html

Said, S. M., Aly, M. M. & Abdek-Akher, M. (2013).
Capacity and location effects of wind turbine energy
systems on power systems stability. *International
Journal on Power Engineering and Energy (IJPEE)*,
4(1), 343-347. doi:10.5772/55090

Taylor, C. W. (1994). *Power system voltage stability*. New
York, NY: McGraw-Hill.

Waewsak, J., Landry, M. & Gagnon, Y. (2015). Offshore
wind power potential of the Gulf of Thailand.
Renewable Energy, 81(C), 609-626. doi:10.1016/j.
renene.2015.03.069.

Wu, Y. -K., Lee, C. -Y., Chou, C. -J. & Liao, W. -M. (2013).
Choice of interconnected points for large-scale
offshore wind farms in Taiwan. *Proceedings of the
2013 CACS International Automatic Control
Conference,* 439–444. doi:10.1109/cacs.2013.6734
175.

Wu, Y.-K., Han, G.-Y., & Lee, C.-Y. (2013). Planning 10
onshore wind farms with corresponding
interconnection network and power system analysis

for low-carbon-island development on Penghu
Island, Taiwan. *Renewable and Sustainable Energy
Reviews*, *19*, 531-540. doi:10.1016/j.rser.2012.10.
043.

Wu, Y.-K., Lee, C.-Y, Chao, H.-Y. & Chang M.-J. (2010).
System impact study for the future large-scale
offshore wind farm around Penghu Archipelago.
*Proceedings of the 2010 International Conference
on Power System Technology* (*POWERCON*), 1–8.
doi:10.1109/POWERCON.2010.5666517

Wu, Y.-K., Lee, C.-Y. & Shu, G.-H. (2011). Taiwan's first
large-scale offshore wind farm connection-a real
project case study with a comparison of wind
turbine. *IEEE Transaction of. Industrial
Application, 47*(3), 1461–1469, 2011. doi:10.1109/
tia.2011.2125933.

Wu, Y.-K., Lee, C.-Y., Chen, C.-R. & Tsai, S.-H. (2011).
Onshore wind farm planning and system simulation
analysis under low-carbon-island project at Penghu.
*Proceedings of the International Conference on
Intelligent System Application to Power Systems
(ISAP)*, 1-7. doi:10.1109/isap.2011.6082178.

Zamora, R. D., Rosado, M. A. (2014). Stability analysis of
wind energy generation in the electrical system of
Puerto Rico. *Proceedings of the International
Conference on Renewable Energies and Power
Quality (ICREPQ' 14)*. doi:10.24084/repqj 12.388.